



# Synthesis, characterization and fluorescence properties of Eu(III) and Tb(III) complexes with novel mono-substituted $\beta$ -diketone ligands and 1,10-phenanthroline

Yi-Ming Luo\*, Jun Li, Lin-Xiang Xiao, Rui-Ren Tang, Xin-Cun Tang

College of Chemistry and Chemical Engineering, Central South University, Changsha 410083, PR China

## ARTICLE INFO

### Article history:

Received 2 June 2008

Received in revised form 30 October 2008

Accepted 31 October 2008

### Keywords:

Mono- $\beta$ -diketone

1,10-Phenanthroline

Eu(III) and Tb(III) complexes

Synthesis

Fluorescence

## ABSTRACT

Two novel pyridine-2,6-dicarboxylic acid derivatives of mono- $\beta$ -diketone, methyl 6-benzoylacetyl-2-pyridinecarboxylate (MBAP) and 6-benzoylacetyl-2-pyridinecarboxylic acid (BAPA) and their Eu(III) and Tb(III) complexes were synthesized and characterized by elemental analysis, FT-IR,  $^1\text{H}$  NMR and TG-DTG. Moreover, their Eu(III) and Tb(III) complexes using 1,10-phenanthroline as a secondary ligand were prepared and characterized. The luminescence properties of these complexes in solid state were investigated in detail. The results suggested that Tb(III) complexes exhibit more efficient luminescence than Eu(III) complexes, the fluorescence intensity of Ln(III) complexes with BAPA is about twice as strong as that of Ln(III) complexes with MBAP, the fluorescence of mono- $\beta$ -diketone complexes using 1,10-phenanthroline as a secondary ligand was prominently higher than that of complexes without adding 1,10-phenanthroline, and the ligand BAPA is an excellent sensitizer to Eu(III) and Tb(III) ion.

© 2008 Elsevier B.V. All rights reserved.

## 1. Introduction

Rare earth complexes with  $\beta$ -diketone ligands have attracted considerable attention because of their high and sharply spiked fluorescence emission efficiency, long lifetime, large Stoke's shift caused by the high absorption coefficient of  $\beta$ -diketone structure [1]. This kind of complexes have promising applications in material science such as luminescent probes [2], sensory materials [3] and organic light-emitting devices (OLEDs) [4–6]. Many  $\beta$ -diketone-type ligands and their lanthanide complexes have been reported and investigated such as butyl methoxy-dibenzoyl-methane, *N*-(2-amino-6-methyl-pyridinyl)ketoacetamide (BMDM), 3-[3-5-bis(phenylmethoxy)phenyl]-1-(9-phenanthryl-1)propane-1,3-dione (PPD), 1-phenyl-3-methyl-4-(4-butylbenzoyl)-5-pyrazolone (HPMBBP) and thenoyltrifluoroacetone (HTTA) [7–11], however, either their absorption coefficients of the optical transitions for these ions are low, or the thermal stability and mechanical properties of the complexes are poor, which limits their practical application considerably.

With an aim to develop novel optical materials, in recent years, some rare earth complexes with  $\beta$ -diketone, aromatic carboxylic acid and heterocyclic carboxylic acid group were under development, such as benzoyl acetone (BA) [12] and

pyridine-2,6-dicarboxylic acid (DPA) [13]. Our group has designed and prepared two pyridine-2,6-dicarboxylic acid derivative ligands of bis- $\beta$ -diketone, and found that their Eu(III) and Tb(III) complexes display relatively weak fluorescence intensity [14,15], in an attempt to increase the fluorescence intensity of the lanthanide complexes, in this paper, two novel pyridine-2,6-dicarboxylic acid derivatives of mono- $\beta$ -diketone named methyl 6-benzoylacetyl-2-pyridinecarboxylate (MBAP) and 6-benzoylacetyl-2-pyridinecarboxylic acid (BAPA) and their Eu(III) and Tb(III) complexes were synthesized. Both of the two novel mono- $\beta$ -diketone ligands have rigid conjugated planar structure, carboxylate group or carboxyl group, which would be of potential applications in time-resolved fluoroimmunoassay and DNA probe. In addition, we prepared Eu(III) and Tb(III) mono- $\beta$ -diketone complexes using 1,10-phenanthroline as a secondary ligand since 1,10-phenanthroline is widely used as assistant antenna groups for photosensitising lanthanide ion. The luminescence properties of all these complexes in solid state were investigated in detail. The synthetic route of ligands is listed in Scheme 1.

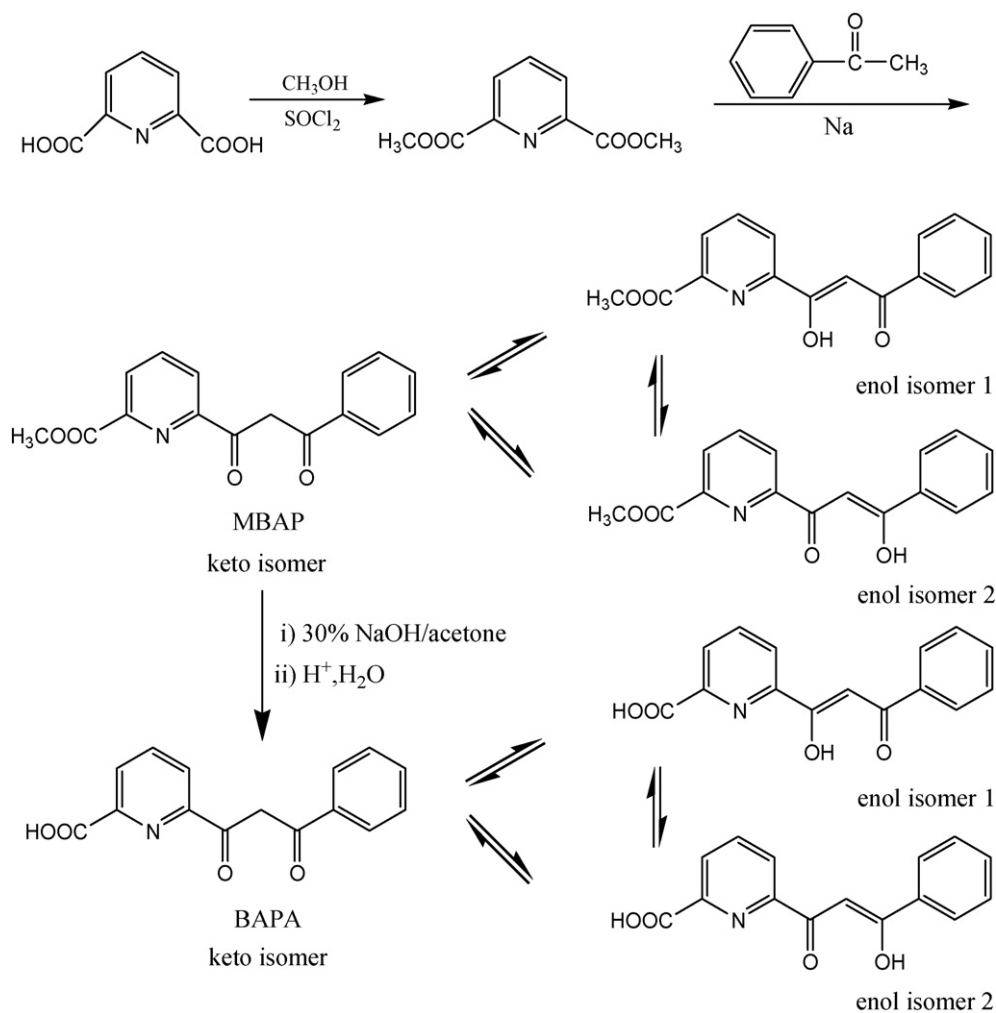
## 2. Experimental

### 2.1. Materials

All starting materials were of AR grade and used without further purification except that rare earth chlorides and dimethyl 2,6-

\* Corresponding author. Fax: +86 731 8879616.

E-mail address: [ymluo@mail.csu.edu.cn](mailto:ymluo@mail.csu.edu.cn) (Y.-M. Luo).



**Scheme 1.** Synthesis of the ligands (MBAP and BAPA).

pyridinedicarboxylate were prepared according to the literature methods [16–18]. Solvents were purified with conventional methods.

## 2.2. Instrumentation

Melting points were determined on a XR-4 apparatus (thermometer uncorrected). Elemental analysis (C, H, N) was performed on a Elemental vario EL elemental analyzer. The lanthanide content was determined by EDTA titration. Infrared spectra were recorded on a Nicolet NEXUS 670 FTIR spectrometer between KBr plates in the range of 4000–400  $\text{cm}^{-1}$ .  $^1\text{H}$  NMR spectra were measured with a Bruker-400 MHz nuclear magnetic resonance instrument using  $\text{CDCl}_3$  as solvent and TMS as internal reference. Thermogravimetric (TG) and differential thermal gravimetry (DTG) were performed in the nitrogen atmosphere using a Shimadzu DTG 40 system at a heating rate of  $10^\circ\text{C min}^{-1}$  from  $30^\circ\text{C}$  to  $700^\circ\text{C}$ . Fluorescence measurements were made on a Hitachi F-4500 spectrometer, the excitation and emission slit widths were 5 nm and 2.5 nm, respectively with PMT voltage at 400 V.

## 2.3. Synthesis of methyl 6-benzoylacetyl-2-pyridinecarboxylate

Flaky sodium (0.69 g, 0.03 mol) was added to a solution of dimethyl 2,6-pyridinedicarboxylate (5.9 g, 0.03 mol) in dry toluene (70 ml), and then acetophenone (0.36 g, 0.03 mol) in dry toluene

(10 ml) was added dropwise under stirring at  $60^\circ\text{C}$  for 4 h [19], the red precipitate was filtered and a yellow solid obtained was washed with petroleum ether to remove unreacted starting material. Addition of aqueous HCl (15 ml, 2 mol/l) led to precipitation of yellow powder which was washed well with water. Recrystallization from ethyl acetate gave a yellow crystal, which was dried in a vacuum. Yield: (6.3 g, 73.7%). m.p.  $116\text{--}118^\circ\text{C}$ . Elemental analytical (calc.) C% 67.53 (67.84), H% 4.62 (4.59), N% 4.88 (4.94). IR (KBr, pellet):  $\nu_{\text{max}}$  ( $\text{cm}^{-1}$ ): 3424 (C=C–OH), 3065 (Ar–H), 2947 ( $\text{CH}_2$ ), 1753 ( $\text{CH}_3\text{OC=O}$ ), 1720 (diketone C=O), 1601, 1570 (C=C, C=N)Ar, 1448, 1433 (C=C, C=N)Ar;  $^1\text{H}$  NMR (400 MHz,  $\text{CDCl}_3$ ): 16.5 (s, 1H, C=C–OH), 8.04–8.32 (m, 3H,  $\text{C}_5\text{H}_3\text{N}$ ), 7.25–7.75 (m, 5H,  $\text{C}_6\text{H}_5$ ), 7.14 (s, 1H, –CH=), 4.03 (s, 3H,  $\text{OCH}_3$ ).

## 2.4. Synthesis of 6-benzoylacetyl-2-pyridinecarboxylic acid

To a solution of methyl 6-benzoylacetyl-2-pyridinecarboxylate (0.50 g, 1.75 mmol) in acetone (10 ml) was added 30% aqueous NaOH (0.28 g, 7 mmol) under stirring at r.t. for 5 h, the precipitate was filtered and a yellow solid afforded was washed with acetone. Addition of aqueous HCl (15 ml, 2 mol/l) led to precipitation of a yellowish powder which was washed well with water. Recrystallization from ethanol gave a yellowish crystal, which was dried in a vacuum. Yield: (0.45 g, 98%). m.p.  $142\text{--}144^\circ\text{C}$ . Elemental analytical (calc.) C% 66.62 (66.91), H% 4.15 (4.09), N% 5.11 (5.20). IR (KBr, pellet):  $\nu_{\text{max}}$  ( $\text{cm}^{-1}$ ): 3467 (C=C–OH), 3060 (Ar–H), 2884 ( $\text{CH}_2$ ), 1717 (COOH), 1693 (diketone C=O), 1605, 1574 (C=C, C=N)Ar, 1464, 1429

**Table 1**  
Elemental analytical data for the complexes.

Complex	C (%) found(calc.)	H (%) found(calc.)	N (%) found(calc.)	Ln (%) found(calc.)
Eu(MBAP) <sub>3</sub> ·7H <sub>2</sub> O	50.79(51.11)	4.81(4.70)	3.57(3.72)	13.22(13.48)
Eu(MBAP) <sub>2</sub> (Phen)·6H <sub>2</sub> O	52.13(52.48)	4.37(4.57)	5.71(5.57)	15.20(15.11)
Eu(BAPA) <sub>3</sub> ·7H <sub>2</sub> O	50.01(49.76)	4.49(4.33)	3.71(3.87)	14.17(14.01)
Eu(BAPA) <sub>2</sub> (Phen)·6H <sub>2</sub> O	51.67(51.53)	4.34(4.29)	5.52(5.72)	15.28(15.54)
Tb(MBAP) <sub>3</sub> ·7H <sub>2</sub> O	50.35(50.79)	4.53(4.67)	3.81(3.70)	14.19(14.02)
Tb(MBAP) <sub>2</sub> (Phen)·6H <sub>2</sub> O	52.40(52.12)	4.32(4.54)	5.70(5.53)	15.51(15.69)
Tb(BAPA) <sub>3</sub> ·7H <sub>2</sub> O	49.82(49.45)	4.12(4.30)	3.71(3.85)	14.63(14.56)
Tb(BAPA) <sub>2</sub> (Phen)·6H <sub>2</sub> O	51.39(51.17)	4.09(4.26)	5.56(5.68)	16.28(16.14)

(C=C, C=N)Ar; <sup>1</sup>H NMR (400 MHz, CDCl<sub>3</sub>): 16.46 (s, 1H, C=C–OH), 10.7 (s, 1H, COOH), 8.15–8.45 (m, 3H, C<sub>5</sub>H<sub>3</sub>N), 7.42–8.06 (m, 5H, C<sub>6</sub>H<sub>5</sub>), 7.26 (s, 1H, –CH=).

### 2.5. Synthesis of complexes

The complex Eu(MBAP)<sub>3</sub>·7H<sub>2</sub>O was prepared in the following steps. A solution of methyl 6-benzoylacetyl-2-pyridinecarboxylate (0.59 g, 2.1 mmol) in ethanol (10 ml) was added dropwise to a solution of Eu(Cl)<sub>3</sub>·6H<sub>2</sub>O (0.26 g, 0.7 mmol) in ethanol (10 ml) under stirring at 60 °C for 24 h. Then the pH value of the mixture was adjusted to 6 by adding an aqueous solution of sodium hydroxide (5%), the green precipitate obtained was separated by filtration, washed three times with ethanol and dried in vacuum for 48 h. The yield was about 61% based on the amount of EuCl<sub>3</sub> used.

The complex Eu(MBAP)<sub>2</sub>(Phen)·6H<sub>2</sub>O was prepared as follows: 1,10-phenanthroline (0.13 g, 0.7 mmol) in ethanol (10 ml) was added to a solution prepared as described for Eu(MBAP)<sub>3</sub>·7H<sub>2</sub>O above. The mixture was heated under stirring at 60 °C for 24 h. Then the pH value of the mixture was adjusted to 6 by adding an aqueous solution of sodium hydroxide (5%). The green precipitate obtained was filtered, washed three times with ethanol and dried in vacuum for 48 h, yield: 69%.

Similarly, the other six complexes Eu(BAPA)<sub>3</sub>·7H<sub>2</sub>O, Eu(BAPA)<sub>2</sub>(Phen)·6H<sub>2</sub>O, Tb(MBAP)<sub>3</sub>·7H<sub>2</sub>O, Tb(MBAP)<sub>2</sub>(Phen)·6H<sub>2</sub>O, Tb(BAPA)<sub>3</sub>·7H<sub>2</sub>O, and Tb(BAPA)<sub>2</sub>(Phen)·6H<sub>2</sub>O were prepared.

All complexes are soluble in DMF, DMSO and methanol, a little soluble in ethanol, ethyl acetate and acetone, insoluble in benzene, diethyl ether and THF.

## 3. Results and discussion

### 3.1. Elemental analysis

Analytical data for the complexes were presented in Table 1. The results of elemental analysis indicated that the composition of the complexes conforms to Ln(MBAP)<sub>3</sub>·7H<sub>2</sub>O, Ln(MBAP)<sub>2</sub>(Phen)·6H<sub>2</sub>O, Ln(BAPA)<sub>3</sub>·7H<sub>2</sub>O, and Ln(BAPA)<sub>2</sub>(Phen)·6H<sub>2</sub>O.

### 3.2. Infrared spectra

The IR spectral data of the ligands and their lanthanide(III) complexes were listed in Table 2. In the ligands of MBAP and BAPA, we observed broad weak bands with fine structure at 3424 cm<sup>-1</sup> and 3467 cm<sup>-1</sup> which can be attributed to the C=C–OH. In addition, high intensity sharp bands are observed at 1753 cm<sup>-1</sup>, 1720 cm<sup>-1</sup> in MBAP and 1717 cm<sup>-1</sup>, 1693 cm<sup>-1</sup> in BAPA which are attributed to the ROC=O and β-diketone C=O, respectively. The high intensity bands at 1601 cm<sup>-1</sup> in MBAP and 1605 cm<sup>-1</sup> in BAPA were assigned to C=C. These bands confirm the presence of the aromatic ring. Medium intensity bands in the 1574–1491 cm<sup>-1</sup> region were regarded as a combination of C=N of the pyridine ring and aromatic C=C stretching vibrations. High intensity bands appearing at 1304 cm<sup>-1</sup> in MBAP and 1318 cm<sup>-1</sup> in BAPA were assigned to the C–O vibration from C=C–O.

In the case of Ln(III) complexes we observed the following changes. All the complexes exhibited broad medium intensity bands at about 3364 cm<sup>-1</sup>, which were assigned to the coordinated water molecule. The high intensity bands appearing around 1753 cm<sup>-1</sup> in MBAP and 1717 cm<sup>-1</sup> in BAPA, which were ascribed to ROC=O, downshifted to 1608 cm<sup>-1</sup> in the Ln(III) complexes, this confirms that the oxygen atoms of ROC=O coordinated to Ln(III) ions successfully. The high intensity bands appearing around 1572 cm<sup>-1</sup> in MBAP and 1574 cm<sup>-1</sup> in BAPA, due to C=N in pyridine ring, downshifted to about 1522 cm<sup>-1</sup> and 1524 cm<sup>-1</sup> in these Ln(III) complexes. The obvious shifts indicated that the C=N groups of the ligands coordinated to the Ln(III) ions through nitrogen atoms. The high intensity bands due to C–O vibration from C=C–O appearing at 1304 cm<sup>-1</sup> in MBAP and 1318 cm<sup>-1</sup> in BAPA downshifted to around 1287 cm<sup>-1</sup> and 1285 cm<sup>-1</sup> in the Ln(III) complexes, which confirms that the enol hydroxyl groups reacted with Ln(III) ions via deprotonation. The complexes showed medium intensity bands in the region 562–594 cm<sup>-1</sup> which was assigned to Ln–N [20,21] and 423–437 cm<sup>-1</sup> assigned to Ln–O modes [22].

According to the results above, we reached the conclusion that the ligands coordinated to the Ln(III) ions via the oxygen atoms of the carbonyl, enol hydroxyl groups and the nitrogen atoms of the pyridine ring and 1,10-phenanthroline. The elemental analysis

**Table 2**  
The most important IR bands of the ligands and their complexes (cm<sup>-1</sup>).

Compound	ν(C–OH)	ν(ROC=O)	ν(C=C)	ν(C=N)	ν(C–O)	ν(Ln–N)	ν(Ln–O)
MBAP	3424	1753	1601	1572	1304		
BAPA	3467	1717	1605	1574	1318		
Eu(MBAP) <sub>3</sub> ·7H <sub>2</sub> O	3338	1609	1570	1521	1287	594	428
Eu(MBAP) <sub>2</sub> (Phen)·6H <sub>2</sub> O	3364	1608	1571	1523	1287	562	437
Eu(BAPA) <sub>3</sub> ·7H <sub>2</sub> O	3398	1608	1568	1523	1290	562	430
Eu(BAPA) <sub>2</sub> (Phen)·6H <sub>2</sub> O	3364	1608	1568	1521	1291	562	423
Tb(MBAP) <sub>3</sub> ·7H <sub>2</sub> O	3363	1610	1572	1523	1288	589	439
Tb(MBAP) <sub>2</sub> (Phen)·6H <sub>2</sub> O	3371	1610	1573	1522	1287	596	437
Tb(BAPA) <sub>3</sub> ·7H <sub>2</sub> O	3386	1612	1569	1524	1285	594	436
Tb(BAPA) <sub>2</sub> (Phen)·6H <sub>2</sub> O	3396	1615	1571	1523	1283	593	436

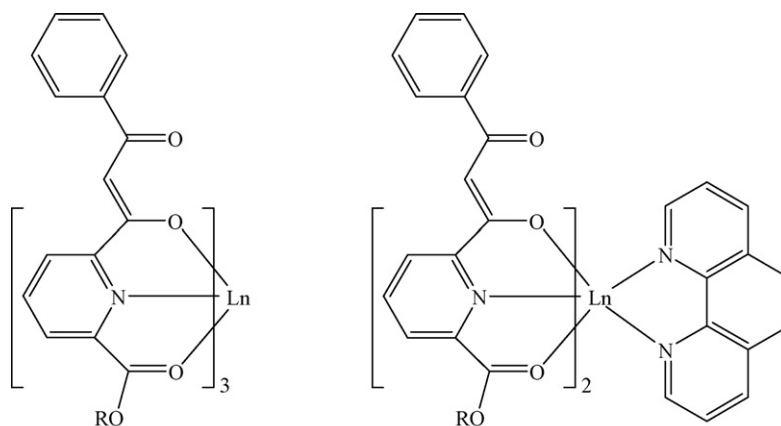


Fig. 1. Chemical structures of the complexes.

**Table 3**  
Fluorescence data for the complexes.

Complex	Slit (nm)	$\lambda_{\text{ex}}$ (nm)	$\lambda_{\text{em}}$ (nm)	RFI	Assignment
Eu(MBAP) <sub>3</sub> ·7H <sub>2</sub> O	5	281	592	287	<sup>5</sup> D <sub>0</sub> → <sup>7</sup> F <sub>1</sub>
			619	775	<sup>5</sup> D <sub>0</sub> → <sup>7</sup> F <sub>2</sub>
Eu(MBAP) <sub>2</sub> (Phen)·6H <sub>2</sub> O	5	282	592	673	<sup>5</sup> D <sub>0</sub> → <sup>7</sup> F <sub>1</sub>
			619	1916	<sup>5</sup> D <sub>0</sub> → <sup>7</sup> F <sub>2</sub>
Eu(BAPA) <sub>3</sub> ·7H <sub>2</sub> O	2.5	292	592	3894	<sup>5</sup> D <sub>0</sub> → <sup>7</sup> F <sub>1</sub>
			619	736	<sup>5</sup> D <sub>0</sub> → <sup>7</sup> F <sub>2</sub>
Eu(BAPA) <sub>2</sub> (Phen)·6H <sub>2</sub> O	2.5	312	592	2143	<sup>5</sup> D <sub>0</sub> → <sup>7</sup> F <sub>1</sub>
			619	6581	<sup>5</sup> D <sub>0</sub> → <sup>7</sup> F <sub>2</sub>
Tb(MBAP) <sub>3</sub> ·7H <sub>2</sub> O	2.5	284	493	2144	<sup>5</sup> D <sub>4</sub> → <sup>7</sup> F <sub>6</sub>
			545	4102	<sup>5</sup> D <sub>4</sub> → <sup>7</sup> F <sub>5</sub>
Tb(MBAP) <sub>2</sub> (Phen)·6H <sub>2</sub> O	2.5	293	493	3218	<sup>5</sup> D <sub>4</sub> → <sup>7</sup> F <sub>6</sub>
			545	5795	<sup>5</sup> D <sub>4</sub> → <sup>7</sup> F <sub>5</sub>
Tb(BAPA) <sub>3</sub> ·7H <sub>2</sub> O	2.5	301	493	5519	<sup>5</sup> D <sub>4</sub> → <sup>7</sup> F <sub>6</sub>
			545	9369	<sup>5</sup> D <sub>4</sub> → <sup>7</sup> F <sub>5</sub>
Tb(BAPA) <sub>2</sub> (Phen)·6H <sub>2</sub> O	2.5	285	493	8124	<sup>5</sup> D <sub>4</sub> → <sup>7</sup> F <sub>6</sub>
			545	>10,000	<sup>5</sup> D <sub>4</sub> → <sup>7</sup> F <sub>5</sub>

and IR spectra results put together lead us to propose the general structures shown in Fig. 1.

### 3.3. Fluorescence studies

The fluorescence characteristics of Eu(III) and Tb(III) complexes in solid state were measured at room temperature under PMT voltage 400 V. Under identical experimental conditions, the fluorescence characteristics of all complexes in solid state were listed in Table 3. The fluorescence spectra of the complexes were shown in Figs. 2–5. In the Eu(III) complexes, we could see that the emission band <sup>5</sup>D<sub>0</sub> → <sup>7</sup>F<sub>2</sub> is obviously higher than the other emission band <sup>5</sup>D<sub>0</sub> → <sup>7</sup>F<sub>1</sub> (Figs. 2 and 3), and in the Tb(III) complexes the emission band <sup>5</sup>D<sub>4</sub> → <sup>7</sup>F<sub>5</sub> is distinctly stronger than the other emission bands <sup>5</sup>D<sub>4</sub> → <sup>7</sup>F<sub>6</sub>, <sup>5</sup>D<sub>4</sub> → <sup>7</sup>F<sub>4</sub> and <sup>5</sup>D<sub>4</sub> → <sup>7</sup>F<sub>3</sub> (Figs. 4 and 5).

It is shown in Figs. 2–5 that the complexes show the characteristic emissions of Eu(III) and Tb(III). Among these eight complexes, it is clearly observed that the fluorescence intensity of Tb(III) complexes with MBAP and BAPA is much stronger than that of corresponding Eu(III) complexes. This is mostly because that the luminescence of Ln(III) complexes is related to the efficiency of the intramolecular energy transfer between the triplet level of the ligands and the emitting level of the ions, which depends on the energy gap between the two levels, probably the energy gap between the ligand triplet levels and the emitting level of Tb(III)

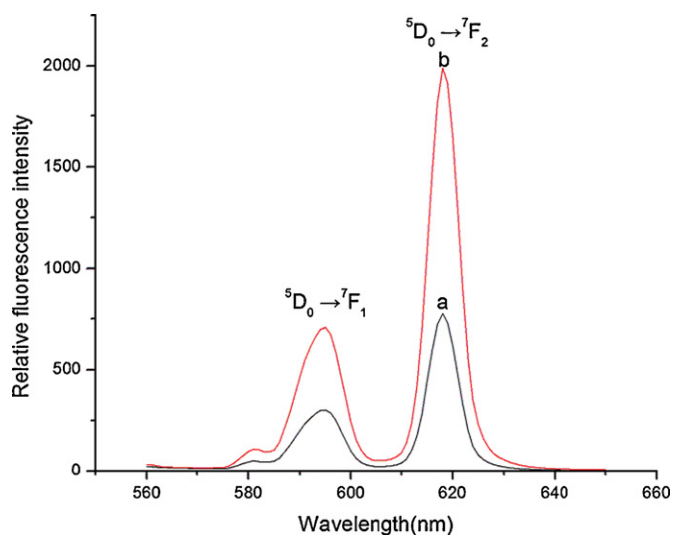
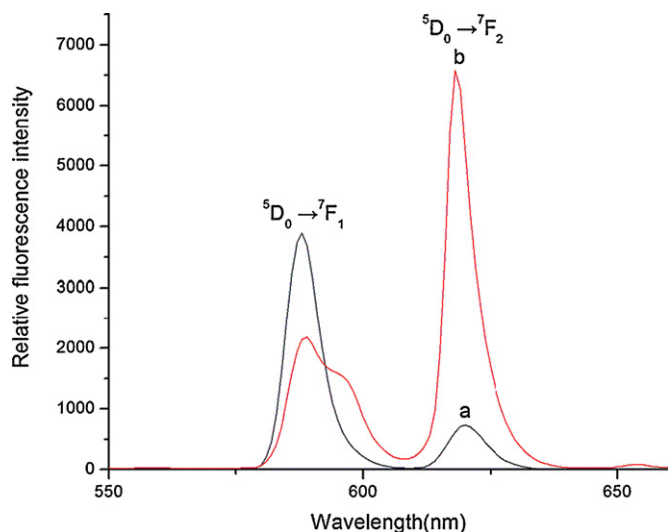


Fig. 2. Fluorescence spectrum of the Eu(MBAP)<sub>2</sub>(Phen)·6H<sub>2</sub>O (b) and Eu(MBAP)<sub>3</sub>·7H<sub>2</sub>O (a) in solid. The excitation and emission slit widths were 5 nm and the PMT voltage was 400 V.



**Fig. 3.** Fluorescence spectrum of  $\text{Eu}(\text{BAPA})_2(\text{Phen})\cdot 6\text{H}_2\text{O}$  (b) and  $\text{Eu}(\text{BAPA})_3\cdot 7\text{H}_2\text{O}$  (a) in solid. The excitation and emission slit widths were 2.5 nm and the PMT voltage was 400 V.

favors to the energy transfer process compared with  $\text{Eu}(\text{III})$  complexes.

In addition, the fluorescence emission of  $\text{Eu}(\text{III})$  and  $\text{Tb}(\text{III})$  complexes using 1,10-phenanthroline as a secondary ligand is at least 40% higher than corresponding complexes without adding 1,10-phenanthroline in each case (Figs. 2–5).

It is also observed that the fluorescence intensity of  $\text{Ln}(\text{III})$  complexes with BAPA is about twice as strong as that of  $\text{Ln}(\text{III})$  complexes with MBAP. Compared with previously reported  $\text{Tb}(\text{III})$  complexes with bis- $\beta$ -diketone-type ligands that we have synthesized [15],  $\text{Tb}(\text{III})$  complexes with BAPA and 1,10-phenanthroline in this paper have slightly higher fluorescence, this could mainly be attributed to the introduction of carboxyl functional group which is beneficial to the energy transfer from the ligands to  $\text{Tb}(\text{III})$  ion.

### 3.4. Thermogravimetric analysis

The two complexes  $\text{Tb}(\text{BAPA})_3\cdot 7\text{H}_2\text{O}$  and  $\text{Tb}(\text{BAPA})_2(\text{Phen})\cdot 6\text{H}_2\text{O}$  were selected to perform thermal decomposition analysis.

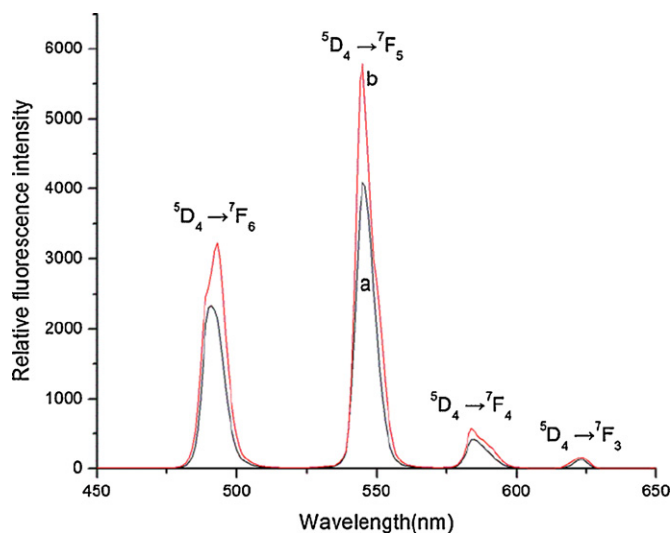


**Fig. 4.** Fluorescence spectrum of the  $\text{Tb}(\text{MBAP})_2(\text{Phen})\cdot 6\text{H}_2\text{O}$  (b) and  $\text{Tb}(\text{MBAP})_3\cdot 7\text{H}_2\text{O}$  (a) in solid. The excitation and emission slit widths were 2.5 nm and the PMT voltage was 400 V.

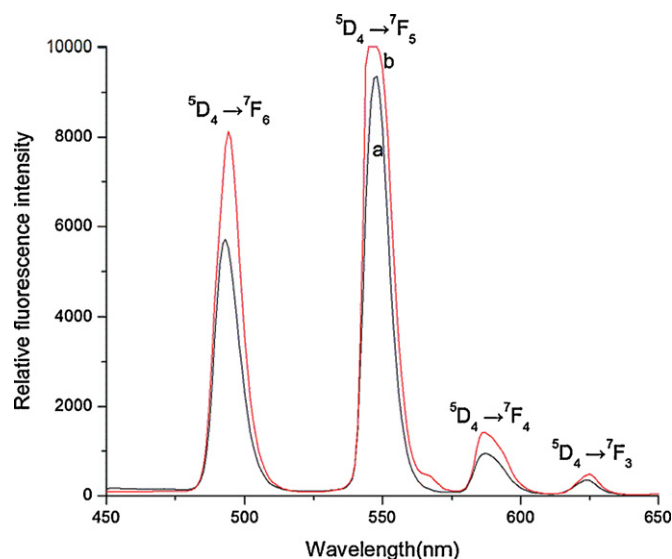


**Fig. 5.** Fluorescence spectrum of the  $\text{Tb}(\text{BAPA})_2(\text{Phen})\cdot 6\text{H}_2\text{O}$  (b) and  $\text{Tb}(\text{BAPA})_3\cdot 7\text{H}_2\text{O}$  (a) in solid. The excitation and emission slit widths were 2.5 nm and the PMT voltage was 400 V.

Figs. 6 and 7 show the thermogravimetric and differential thermal gravimetry curves obtained by heating  $\text{Tb}(\text{BAPA})_3\cdot 7\text{H}_2\text{O}$  and  $\text{Tb}(\text{BAPA})_2(\text{Phen})\cdot 6\text{H}_2\text{O}$  in nitrogen atmosphere with the heating rate of  $10^\circ\text{C}\text{min}^{-1}$ . The decomposition takes place between  $30^\circ\text{C}$  and  $700^\circ\text{C}$ . The thermal analytical data are listed in Table 4. In the TG–DTG curves, there are two main successive mass loss stages from  $30^\circ\text{C}$  to  $700^\circ\text{C}$  for the two complexes. The first mass loss stage of  $\text{Tb}(\text{MBAP})_3\cdot 7\text{H}_2\text{O}$  starts at  $111^\circ\text{C}$ , ends at  $145^\circ\text{C}$  and reaches the largest rate at  $123^\circ\text{C}$  with mass loss percentage of 11.24%, this stage roughly coincides with the value of 11.11%, calculated for the loss of seven water molecules from the complex. Similarly, the first mass loss stage of  $\text{Tb}(\text{MBAP})_2(\text{Phen})\cdot 6\text{H}_2\text{O}$  starts at  $105^\circ\text{C}$ , ends at  $145^\circ\text{C}$  and reaches the largest rate at  $124^\circ\text{C}$  with mass loss percentage of 10.45%, this stage roughly coincides with the value of 10.66%, calculated for the loss of six water molecules from the complex.

The second stage of  $\text{Tb}(\text{MBAP})_3\cdot 7\text{H}_2\text{O}$  with 72.61% mass loss starts at  $445^\circ\text{C}$ , finishes at  $610^\circ\text{C}$  and reaches the largest rate at  $498^\circ\text{C}$ . The mass loss percentage is near the loss of three MBAP molecules from the complex (calc. 72.39%). And the second stage of  $\text{Tb}(\text{MBAP})_2(\text{Phen})\cdot 6\text{H}_2\text{O}$  with 70.49% mass loss starts at  $450^\circ\text{C}$ ,

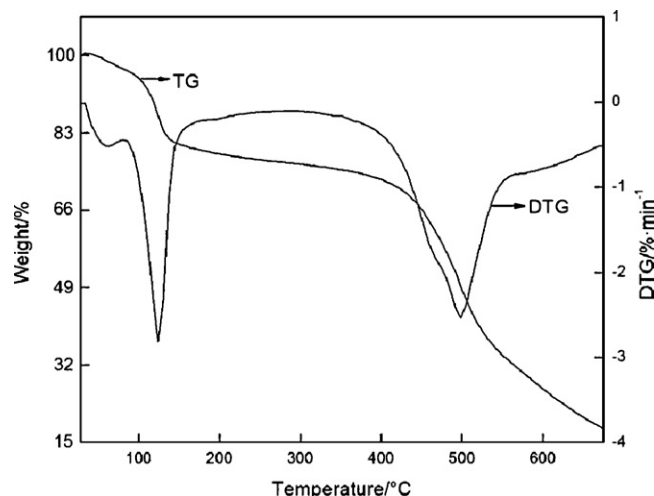


**Fig. 6.** TG–DTG curves of  $\text{Tb}(\text{MBAP})_3\cdot 7\text{H}_2\text{O}$  under  $\text{N}_2$  atmosphere with the heating rate of  $10^\circ\text{C}\text{min}^{-1}$ .

**Table 4**  
Thermal decomposition data for Tb(MBAP)<sub>3</sub>·7H<sub>2</sub>O and Tb(MBAP)<sub>2</sub>(Phen)·6H<sub>2</sub>O.

Complex	Stage	Temperature range (°C)	DTG peak temperature (°C)	Mass loss rate (%) found (calc.)	Probable lost molecules	Intermediate
Tb(MBAP) <sub>3</sub> ·7H <sub>2</sub> O	I	111–145	123	11.24(11.11)	7H <sub>2</sub> O	Tb(MBAP) <sub>3</sub>
	II	445–610	498	72.61(72.39)	3MBAP	Tb <sub>4</sub> O <sub>7</sub>
Tb(MBAP) <sub>2</sub> (Phen)·6H <sub>2</sub> O	I	105–145	124	10.45(10.66)	6H <sub>2</sub> O	Tb(MBAP) <sub>2</sub> (Phen)
	II	450–620	472	70.49(70.87)	2MBAP 1Phen	Tb <sub>4</sub> O <sub>7</sub>

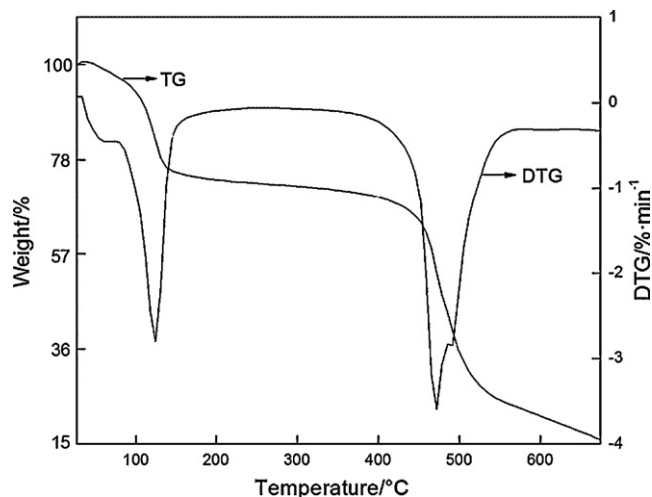
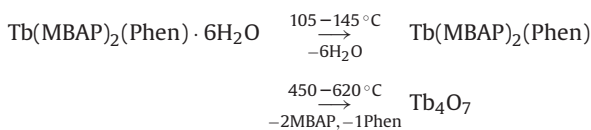
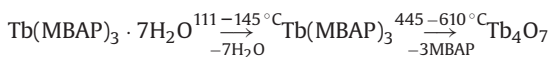


**Fig. 7.** TG–DTG curves of Tb(MBAP)<sub>2</sub>(Phen)·6H<sub>2</sub>O under N<sub>2</sub> atmosphere with the heating rate of 10 °C min<sup>-1</sup>.

finishes at 620 °C and reaches the largest rate at 472 °C. The mass loss percentage is near the loss of two MBAP molecules and one 1,10-phenanthroline molecule from the complex (calc. 70.87%). Further heating the two complexes to higher temperatures results in plateaus in TG curves corresponding to the formation of Tb<sub>4</sub>O<sub>7</sub>.

In conclusion, on the basis of the TG–DTG analysis, the thermal decomposition processes of Tb(MBAP)<sub>3</sub>·7H<sub>2</sub>O and Tb(MBAP)<sub>2</sub>(Phen)·6H<sub>2</sub>O are predicted as follows:



#### 4. Conclusions

The synthesis and fluorescence properties of Eu(III) and Tb(III) complexes with two novel mono-substituted β-diketone-type ligands, methyl 6-benzoylacetyl-2-pyridinecarboxylate, 6-benzoylacetyl-2-pyridinecarboxylic acid and 1,10-phenanthroline were reported. According to the IR spectra data, coordination of

the ligands to Ln(III) ions was occurring at the oxygen atoms of the carbonyl, enol hydroxyl groups and the nitrogen atoms of the pyridine ring and 1,10-phenanthroline. The fluorescence data indicate that Tb(III) complexes with MBAP and BAPA exhibit much higher emission than corresponding Eu(III) complexes and the fluorescence intensity of Ln(III) complexes with BAPA is about twice as strong as that of Ln(III) complexes with MBAP. It is worth noting that addition of 1,10-phenanthroline to the Eu(III) and Tb(III) complexes lead to the formation of complexes with over 40% higher fluorescence emission, in addition, Tb(III) complexes with BAPA emit stronger green emission than Tb(III) complexes with corresponding bis-β-diketone-type ligands we previously reported and would be considered as promising candidates for applications in organic light-emitting devices (OLEDs), sensory materials and luminescent probes.

#### Acknowledgements

This work is financially supported by National Natural Science Foundation of China (no. 20676152) and the Science Foundation of Hunan Province (no. 05JT1022).

#### References

- [1] G.F. de Sa, O.L. Malta, C.D. Donega, A.M. Simas, R.L. Longo, P.A. Santa-Cruz, E.F. da Silva, *Coord. Chem. Rev.* 196 (2000) 300.
- [2] M.R. Robinson, M.B. O'Regnan, G.C. Bazan, *Chem. Commun.* (2000) 1645.
- [3] J. Kido, Y. Okamoto, *Chem. Rev.* 102 (2002) 2357.
- [4] C.W. Tang, S.A. VanSlyke, *Appl. Phys. Lett.* 51 (1987) 913.
- [5] J. Kido, K. Nagai, Y. Okamoto, *J. Alloys Compd.* 30 (1993) 192.
- [6] N. Takada, T. Tsutsui, S. Saito, *Jpn. J. Appl. Phys.* 33 (1994) 863.
- [7] R.D. Adati, et al., *J. Alloys Compd.* 418 (2006) 222.
- [8] X.S. Tai, M.Y. Tan, *Spectrochim. Acta Part A* 61 (2005) 1767.
- [9] X.Z. Jiang, A.K.Y. Jen, G.D. Phelan, D.Y. Huang, *Thin Solid Films* 416 (2002) 212.
- [10] W.G. Zhu, Q. Jiang, Z.Y. Lu, X.Q. Wei, M.G. Xie, D.C. Zou, T. Tsutsui, *Synth. Met.* 111–112 (2000) 445.
- [11] D.D. Cunha, D. Collins, G. Richards, G.S. Vincent, S. Swavey, *Inorg. Chem. Commun.* 9 (2006) 979.
- [12] B. Meshkova Svetlana, *J. Fluoresc.* 10 (4) (2000) 333.
- [13] X.H. Yin, M.Y. Yang, H.H. Shi, J. *Chin. Rare Earth Soc.* 18 (2000) 211.
- [14] Y.M. Luo, Z. Chen, R.R. Tang, L.X. Xiao, H.J. Peng, *Spectrochim. Acta Part A* 69 (2008) 513.
- [15] L.X. Xiao, Y.M. Luo, Z. Chen, J. Li, R.R. Tang, *Spectrochim. Acta Part A: Mol. Biomol. Spectrosc.* 71 (2008) 321.
- [16] A.J. Chandrasekhar, *Imaging Technol.* 16 (1990) 158.
- [17] R.R. Tang, Z.E. Yan, C.C. Guo, *Chem. J. Chin. Univ.* 27 (2006) 472.
- [18] C. Ewan, C. Lynda, R. David, *Tetrahedron* 51 (1995) 10241.
- [19] R.W. Saalfrank, N. Löw, S. Trummer, G.M. Sheldrick, M. Teichert, D. Stalke, *Eur. J. Chem.* (1998) 559.
- [20] J.R. Doring, R. Layton, D.N. Sink, B.R. Mitchell, *Spectrochim. Acta* 21 (1965) 1326.
- [21] K. Ueno, A.E. Martell, *J. Phys. Chem.* 60 (1956) 1270.
- [22] G. Percy, *Spectrochim. Acta* 32A (1976) 1287.